Photoacoustic imaging using microring resonator

Journal seminar

2014/6/18

M1 Takashi Ogura

Introduction

Brain imaging

small blood vessel cannot be imaged

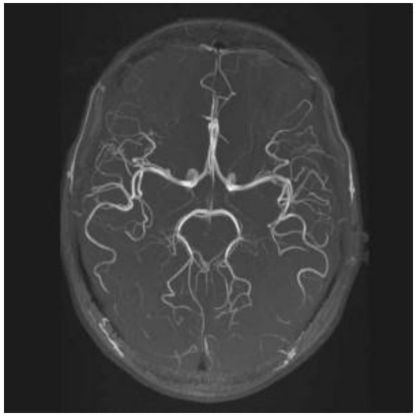

Ref) http://medical-checkup.info/article/49402596.html

Melanoma

Depth is important factor

Ref) Japanese Dermatological Association

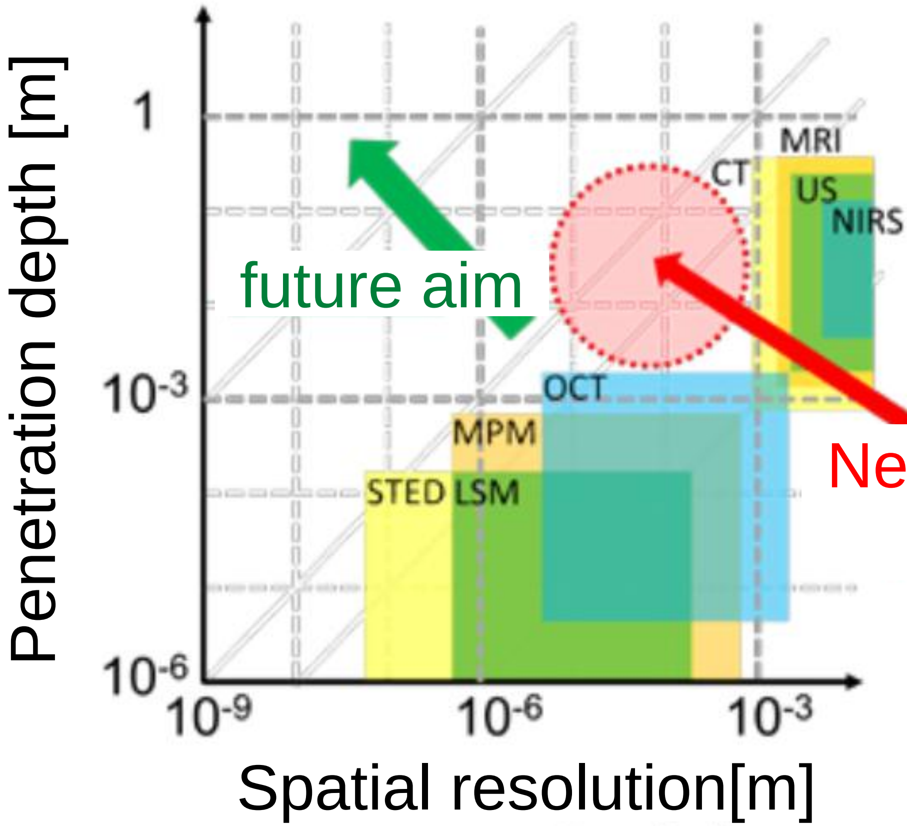

Ref) http://www.jstshingi.jp/abst/p/12/1258/pre/astep022507.pdf

high spatial resolution and penetration depth are important together

Introduction

Photoacoustic microscopy schematic diagram

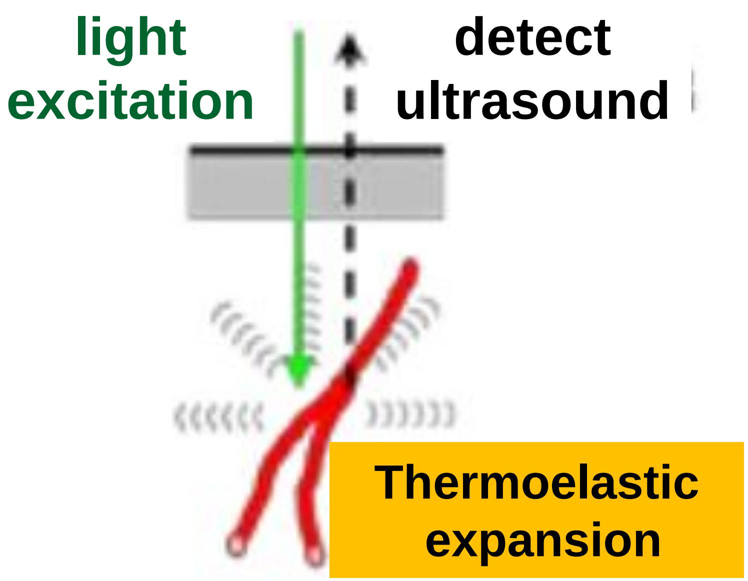

Ref) http://www.jstshingi.jp/abst/p/12/1258/pre/astep022507.pdf

Attenuation coefficient in biological tissue

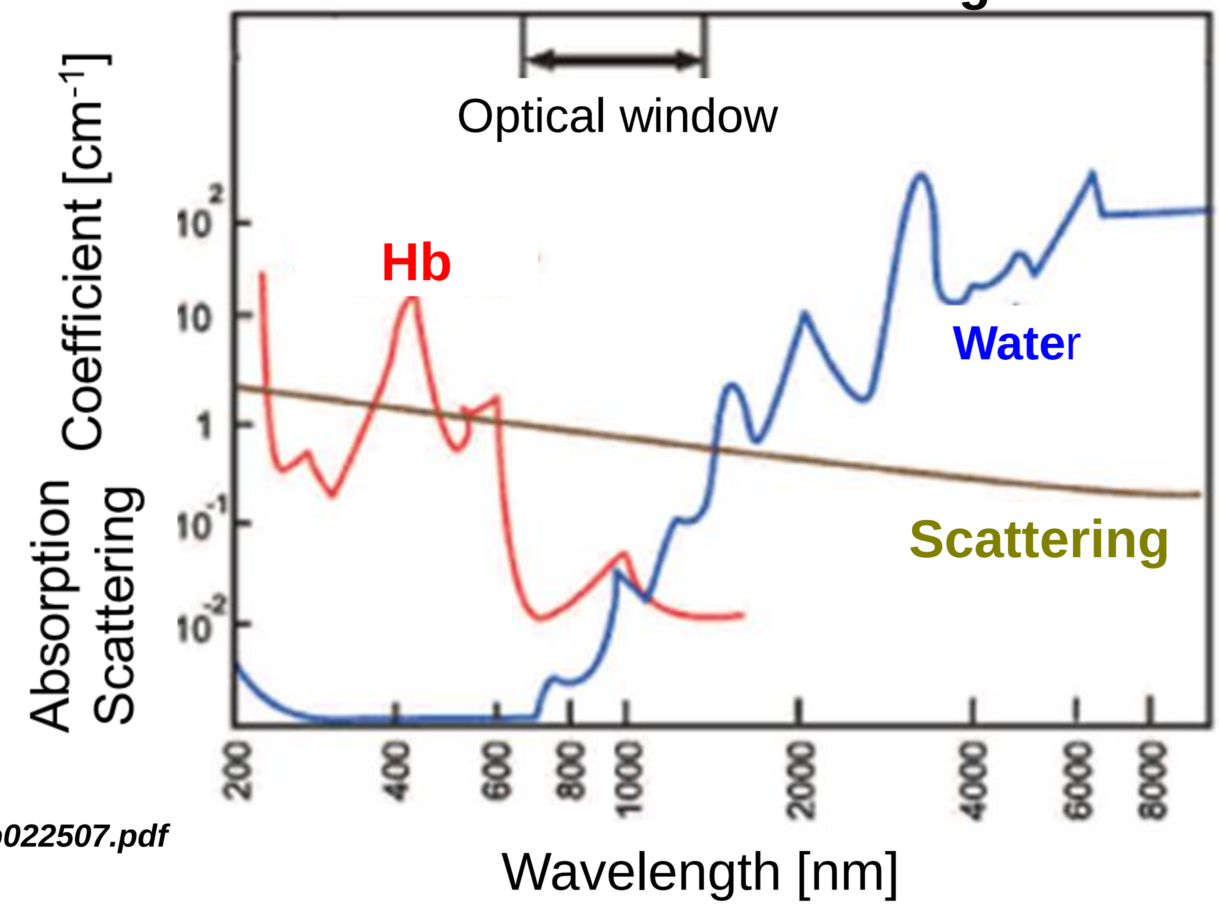

Ultrasound can provide a better resolution than optical imaging in depths greater than ～ 1 mm

Outline

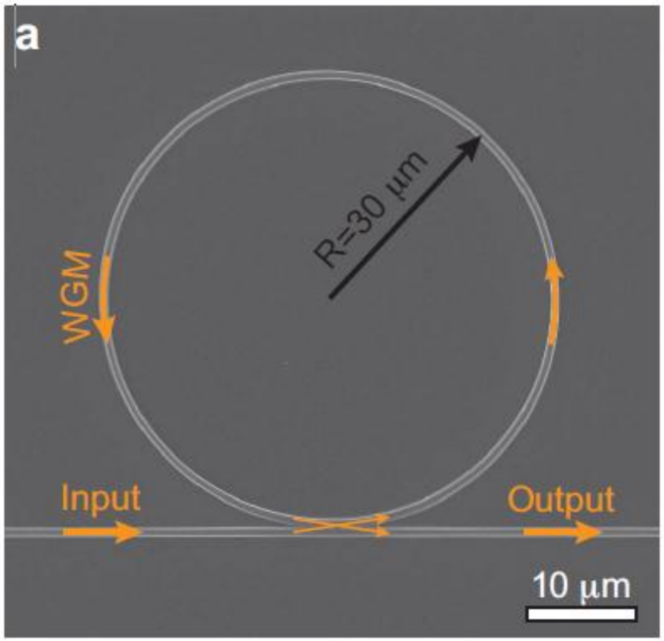

Microring resonator

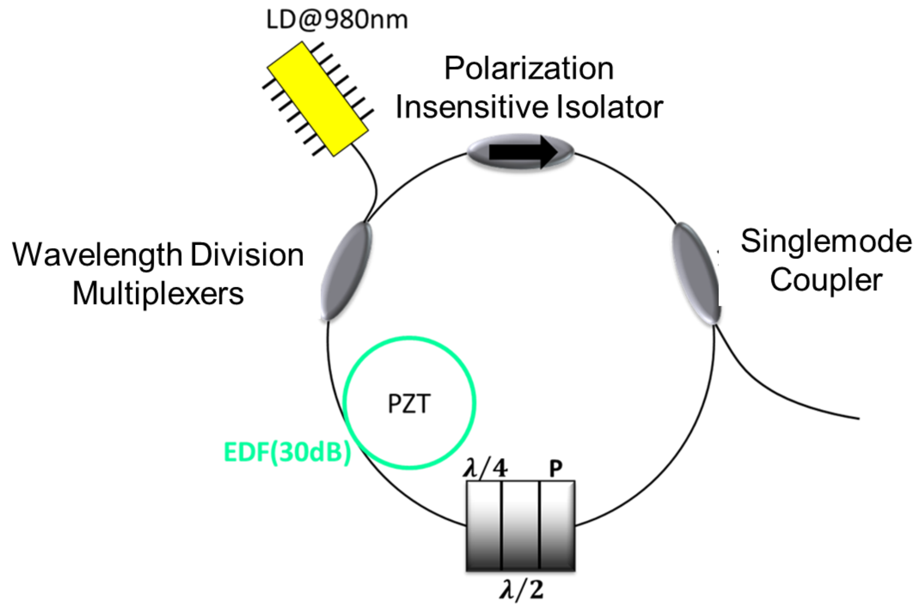

Lab-made mode-locked Er:Fiber laser oscillator

Main Topics

- **Photoacoustic effect principle**
- **Microring resonator(MRR)**
- **Imaging applications**

Absorption

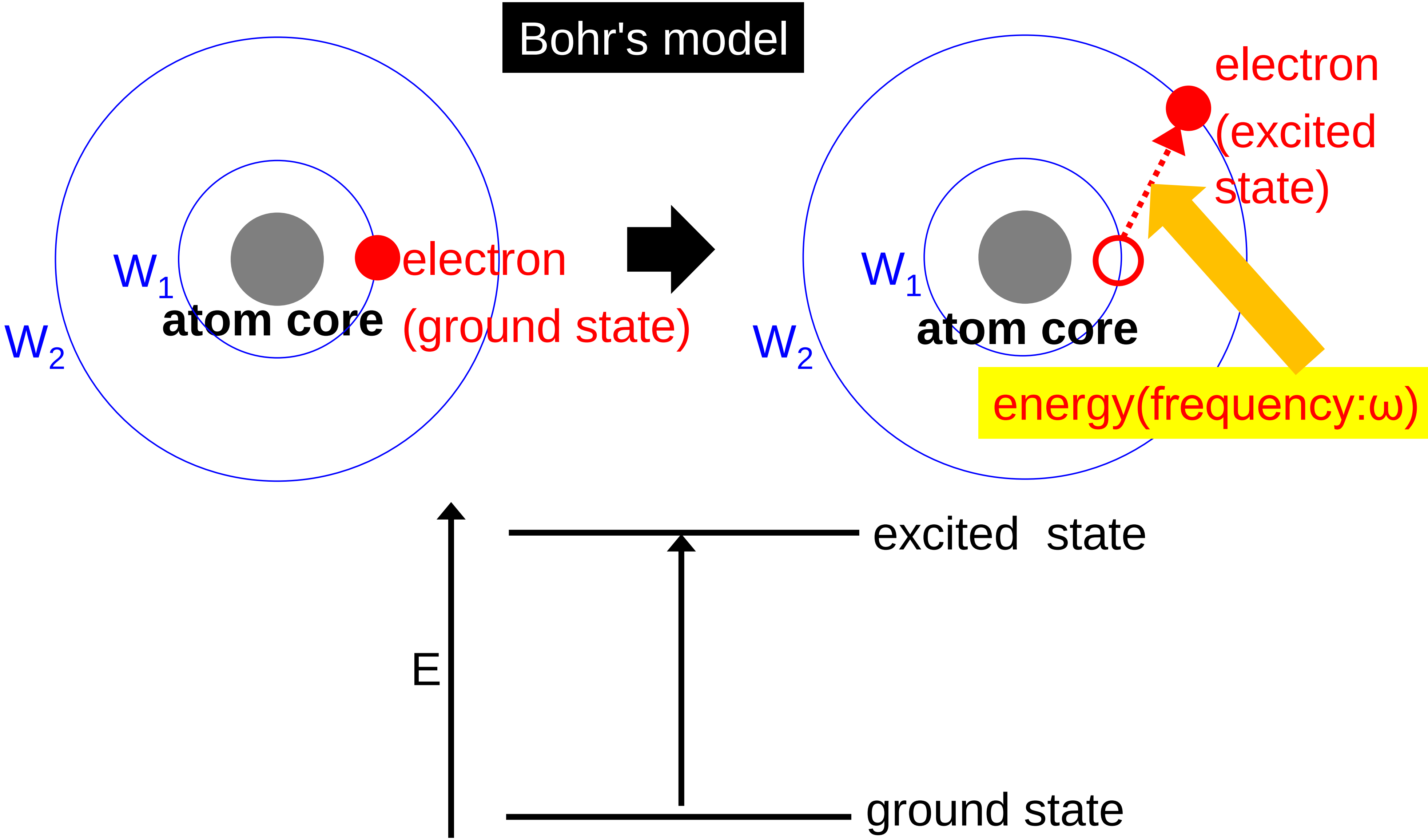
Bohr's model
W_1
W_2
atom core
electron
(ground state)
W_1
W_2
atom core
electron
(excited state)
energy(frequency:ω)
E
excited state
ground state

Deactivation

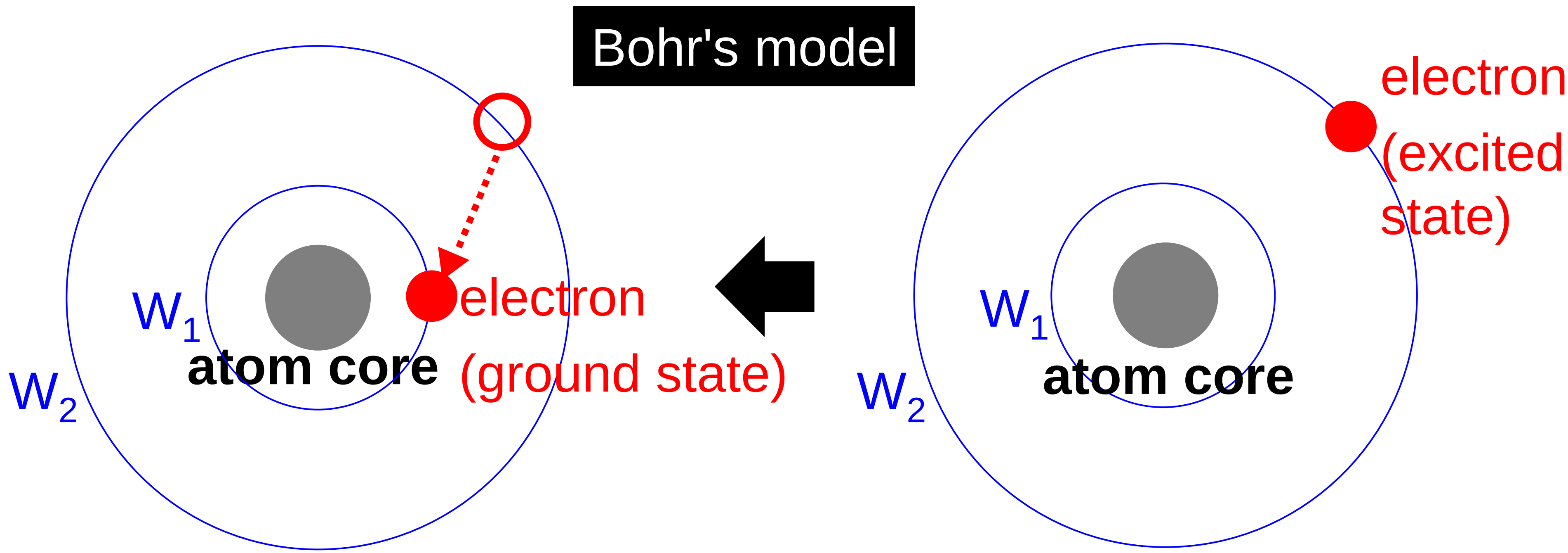

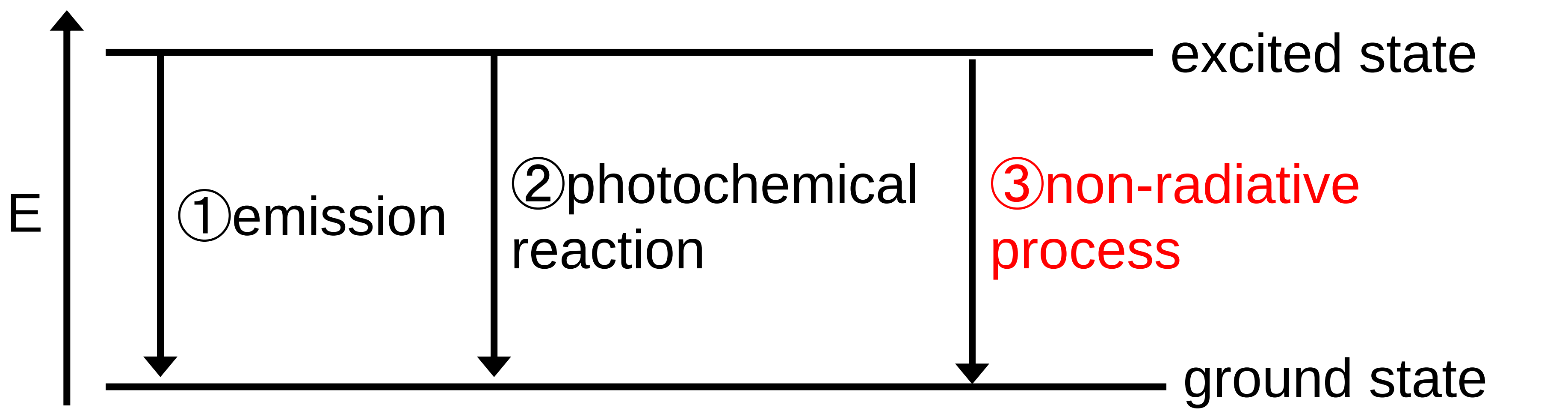

Generation and detection Ultrasound

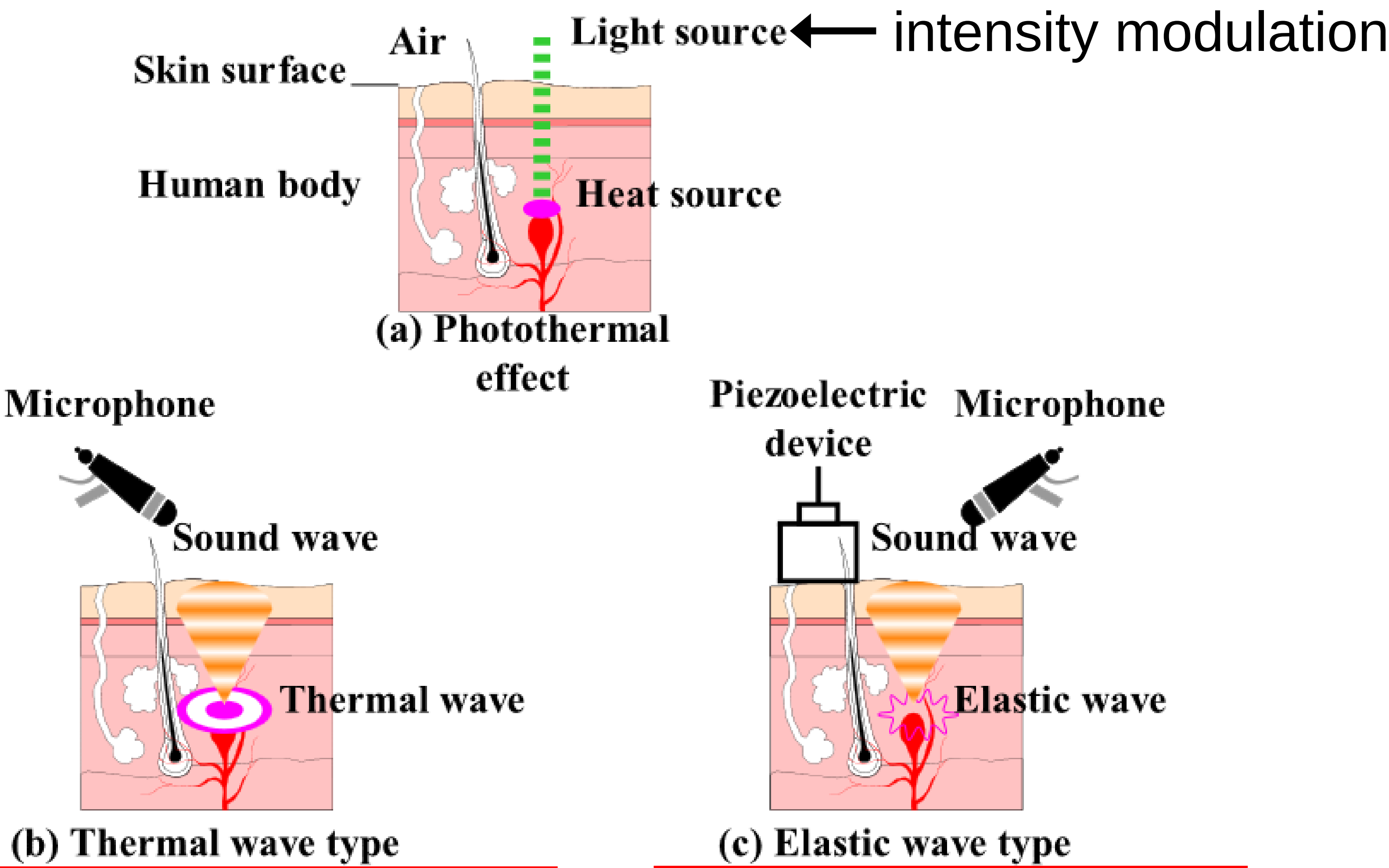

Rosencwaig-Gersho theory

Jackson-Amer theory

History

1880 Alexander Graham Bell first reported the observation of sound generated by light.

1938 Viengerov used the photoacoustic effect for the measurements of light absorption in gases

1970s The development of the laser had critical implications for photoacoustic spectroscopy.

1980s Patel and Tom have established the modern technological basis of the method, by using pulsed lasers as the light source and piezoelectric transducers as the photoacoustic detectors

1. S. W. Huang, S. L. Chen, T. Ling, A. Maxwell, M. O'Donnell, L. J. Guo, and S. Ashkenazi, "Low-noise wideband ultrasound detection using polymer microring resonators" Appl. Phys. Lett. 92,193509 (2008)

2. H. Li, B, Dong, Z. Zhang, H. F. Zhang, and C. Sun, "A transparent broadband ultrasonic detector based on an optical micro-ring resonator for photoacoustic microscopy" Scientific Reports. 4, 4496 (2014)

3. Z. Xie, S. -L. Chen, T, Ling, L. J. Guo, P. L. Carson, X,Wang, "Pure optical photoacoustic microscopy" Opt. Express 19, 9027 (2011)

S. W. Huang, S. L. Chen, T. Ling, A. Maxwell, M. O'Donnell, L. J. Guo, and S. Ashkenazi,

"Low-noise wideband ultrasound detection using polymer microring resonators"

Appl. Phys. Lett. 92,193509 (2008)

Intoroduction

Photoacoustic detector have been often used PVDF
PVDF:Polyvinylidene fluoride

Problem
・increased noise level in small elements
・complexity of electrical interconnects
・fabrication difficulties

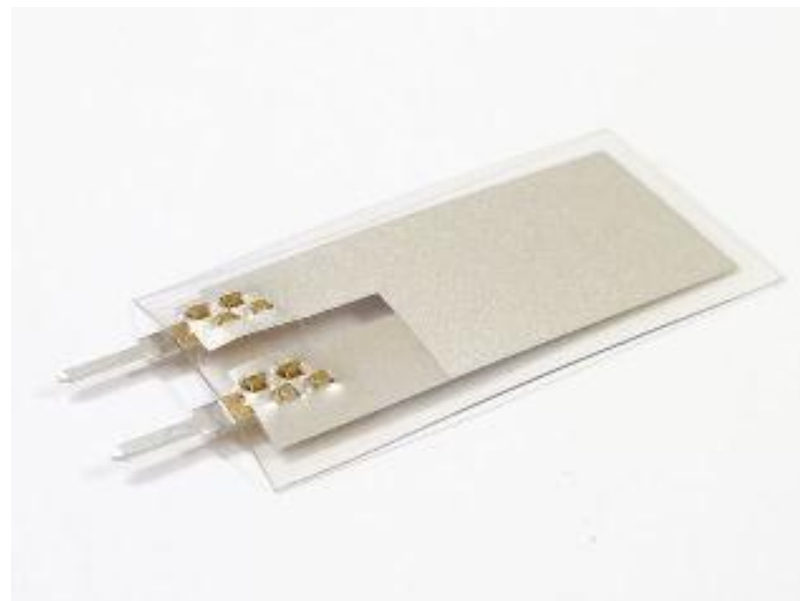

In this letter
・They fabricated polymer microring resonators
・Low noise and high Q factor

Ring resonator

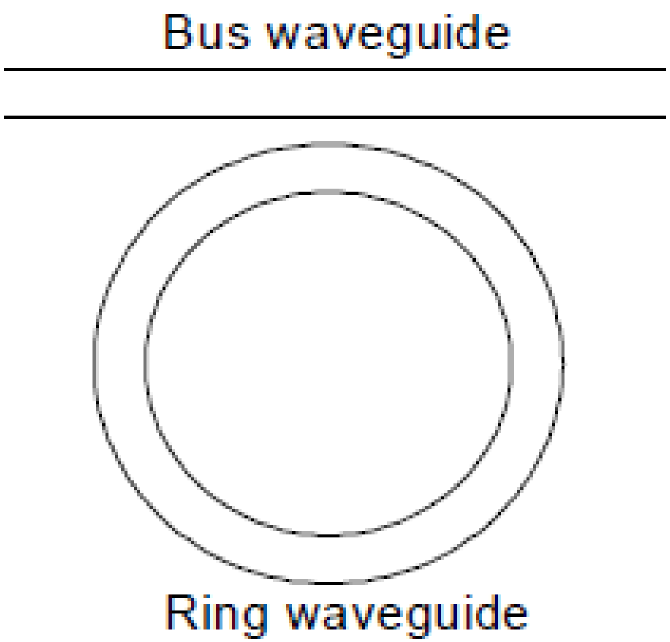

Resonance condition

$$m\lambda_c = n_{eff}L$$

m: resonance order (an integer)
λc: resonance wavelength
n_{eff}: effective index
L: circumference

microring resonator device consists of a straight waveguide coupled with a microring

In microring ultrasound sensors, incident acoustic waves cause a strain field, slightly deforming the waveguide dimension. The change in waveguide cross section directly alters the effective refraction index of the guided mode. Moreover, the refractive indices of the waveguide material and water (surrounding the waveguide) will also be modified by the strain via the elasto-optic effect. Thus, the resonance condition was shifted

Setup

20 MHz unfocused transducer

V316, Panametrics

NDT, Waltham, MA

3.18 mm diameter

WaveSurfer 432, LeCroy, Chestnut Ridge, NY

HP 8168F, Agilent Technologies, Santa Clara, CA

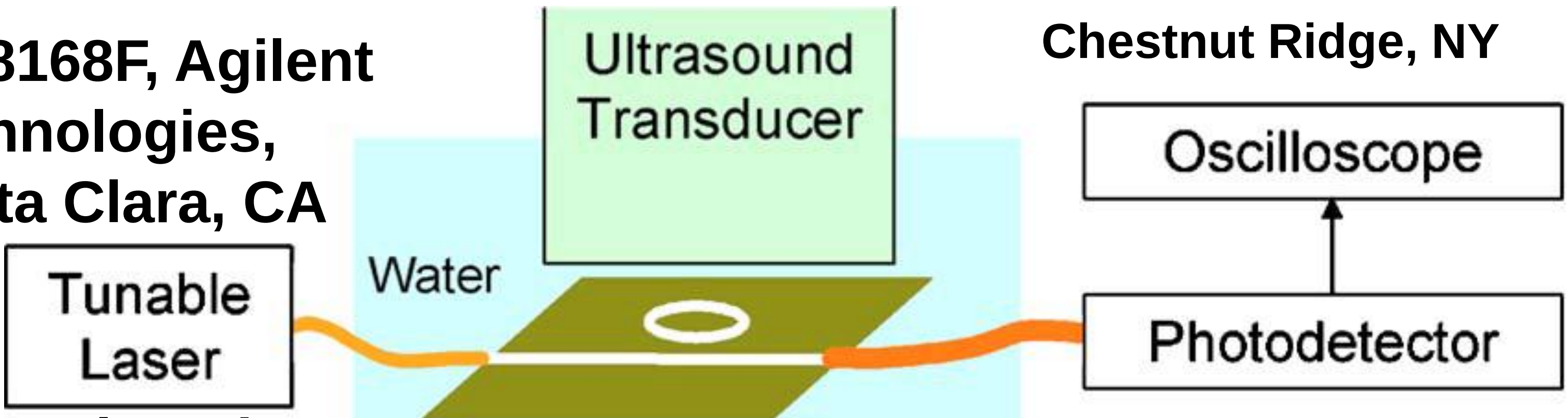

Wavelengths around 1550nm

Microrings diameter:100μm

1811-FC,New Focus, San Jose, CA

dc output gain: 1 V/A

ac output gain: 4 × 10^4 V/A

electrical bandwidth: 25 kHz–125 MHz

Optical transmission spectrum of polymer microring resonator

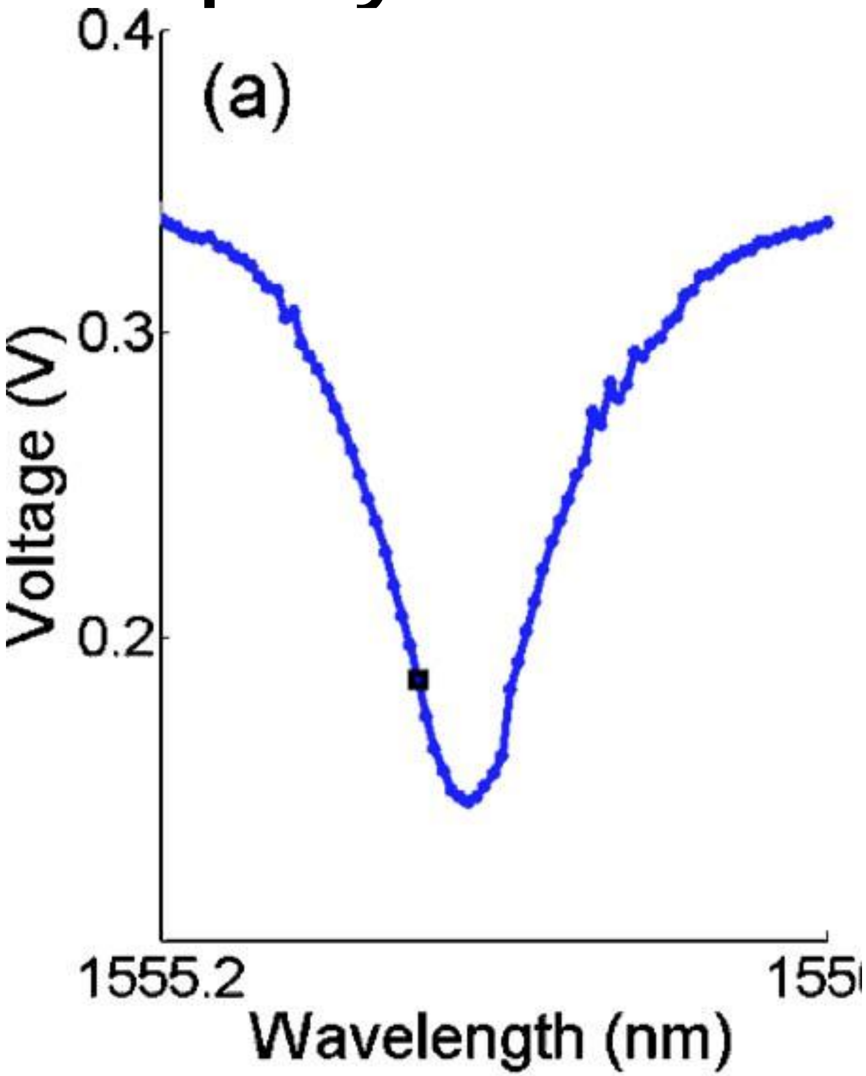

Input power 4.2mW

resonanse wavelength:1555.57nm

half-power bandwidth 0.24nm

$$Q\ factor = \frac{1555.57}{0.24} \approx 6000$$

Single-shot acoustic waveform measured by the resonator

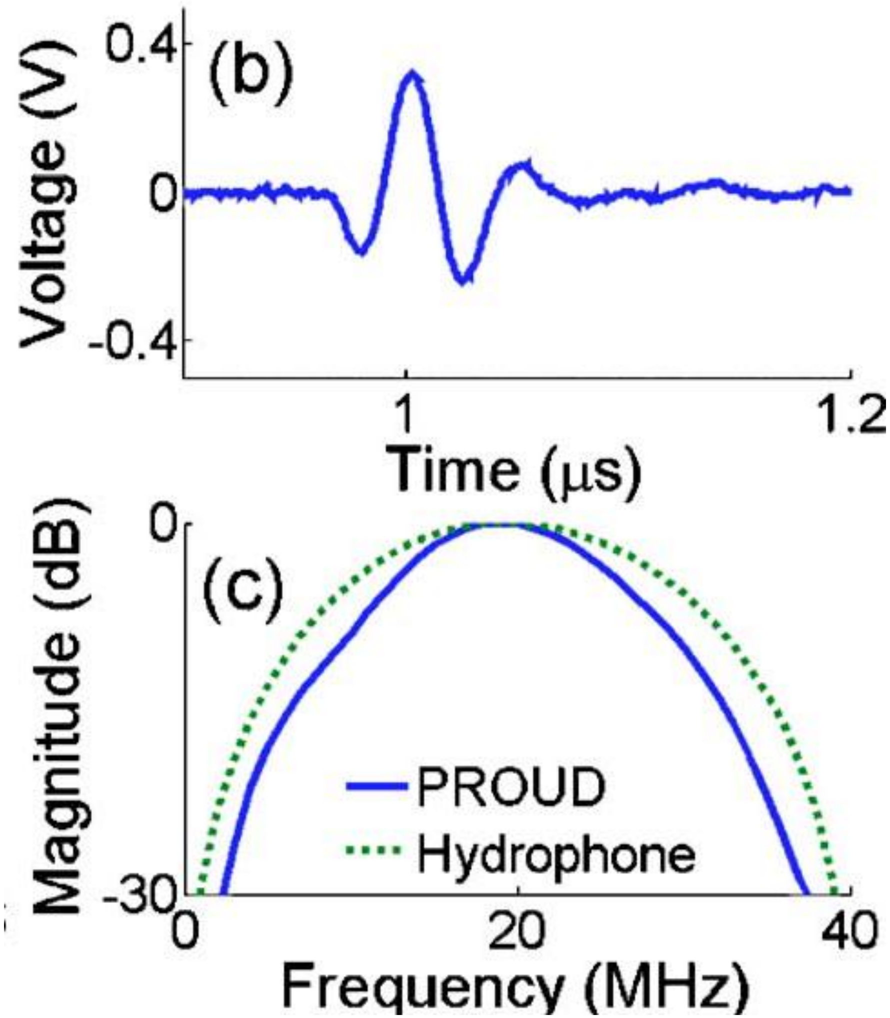

A 20 MHz unfocused transducer outputs a peak pressure of 30 kPa around its surface, calibrated using a hydrophone

The optical probing wavelength and input power were set to

1555.51 nm and 5.5 mW, respectively. Ultrasound signals were detected by the ac output of the photodetector.

Since a 30 kPa acoustic

pressure produced an output voltage of 332 mV, the sensitivity of the PROUD device was 11 mV/ kPa.

NEP(a mesure of the minimum detectable pressure of the device) were 0.14 0.20 0.23kPa

penetration depth

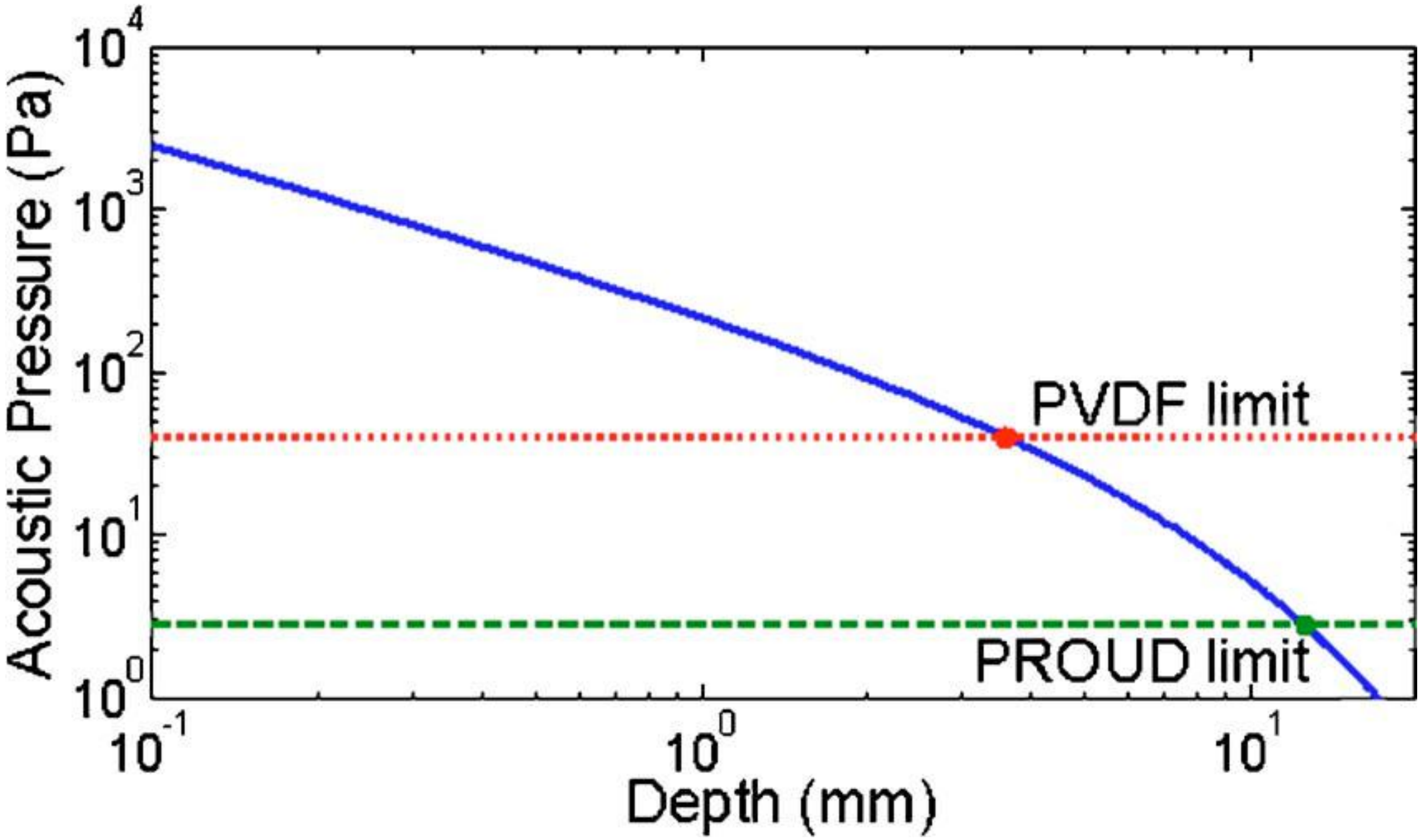

Imaging depths obtained using PROUD and PVDF detector arrays are 12.6 and 3.6 mm, respectively. The depth improvement gained by using PROUD is over threefold.

Summary

- **They fabricated polymer microring resonators with a quality factor of 6000 resulting in high sensitivity to ultrasound.**

- **For a typical photoacoustic imaging test case, the high sensitivity demonstrated in these devices would increase imaging depth by a factor of 3 compared to state-of-the-art polyvinylidene fluoridedetectors.**

H. Li, B, Dong, Z. Zhang, H. F. Zhang, and C. Sun,

“A transparent broadband ultrasonic detector based on an optical micro-ring resonator for photoacoustic

microscopy” Scientific Reports. 4, 4496 (2014)

Intoroduction

Photoacoustic detector have been often used piezoelectric detector

Problem

the sizeable and opaque piezoelectric ultrasonic detectors commonly used in PAM impose a serious constraint

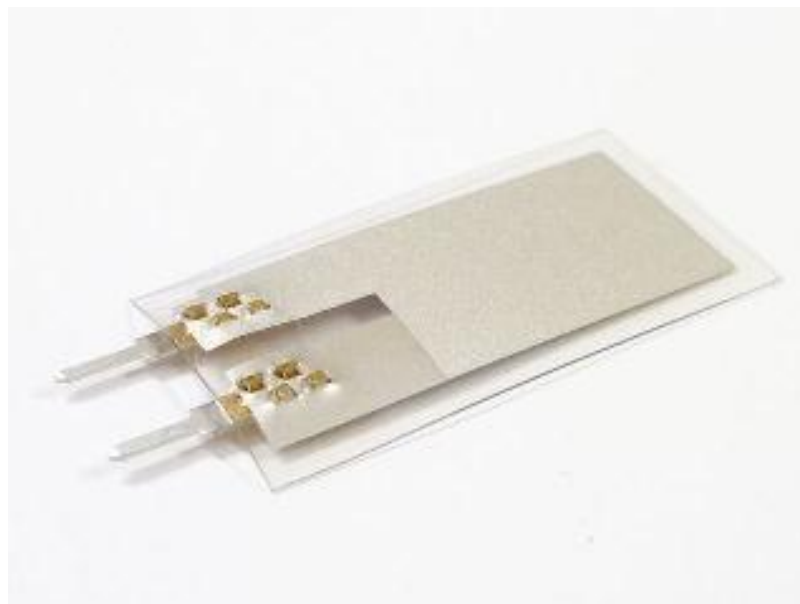

In this letter

・They fabricated microring resonator

・They also established a theoretical framework for designing and optimizing the MRR for PAM.

Setup

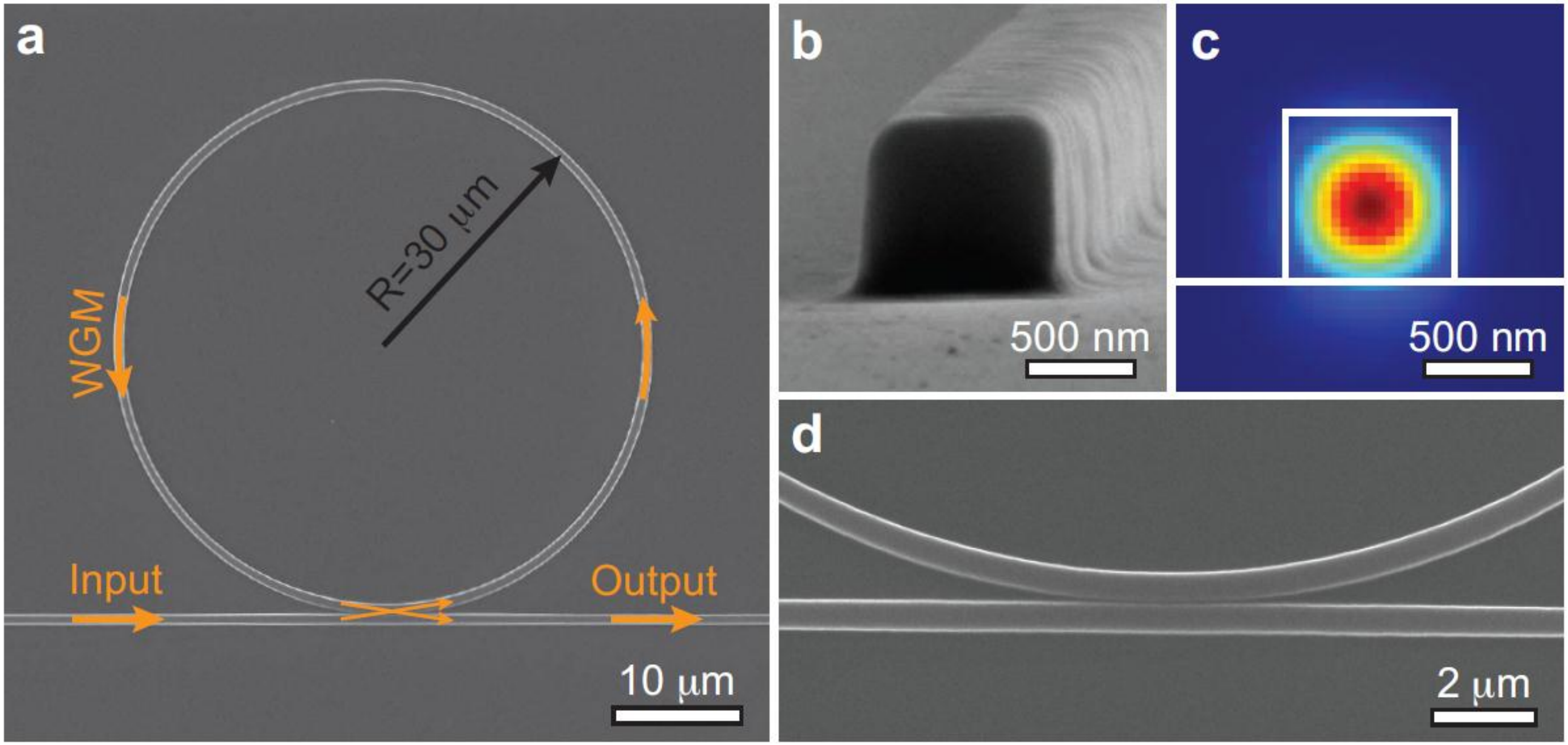

(a) Scanning electron micrograph of the MRR
(b) High-magnification view
(c) Calculated electric field by COMSOL multiphysics
(d) Close-up view of the gap between the ring and bus waveguides.

Transmission spectrum

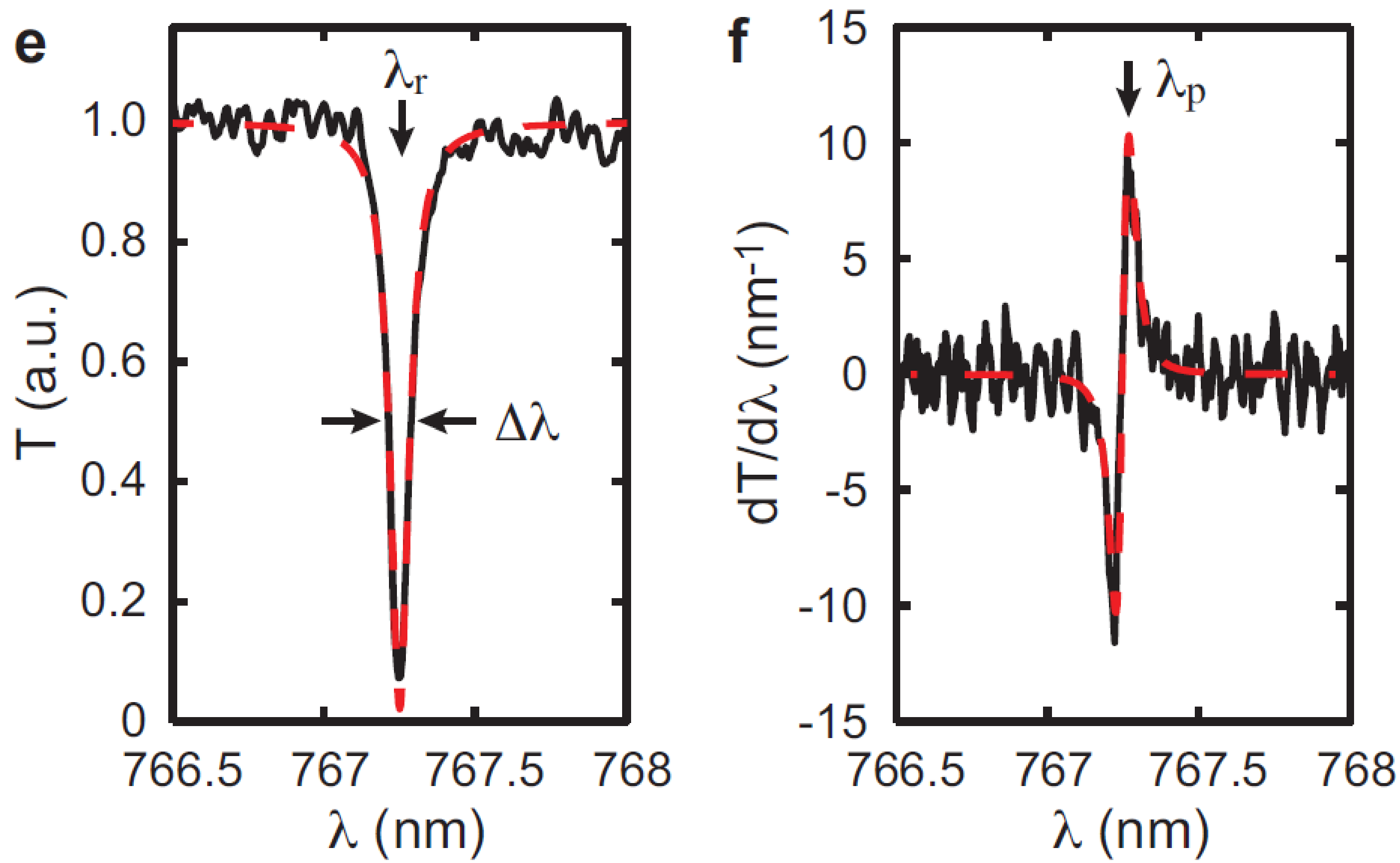

$$Q\ factor = \frac{\lambda_r}{\Delta\lambda} = \frac{767.27 \times 10^3}{73.8} = 10400$$

$\Delta\lambda$: *half − power bandwidth*

λ_r: *resonant frequency*

Sensitivity of detecting pressure

$$S = \frac{dT}{dP} = \frac{dn_{eff}}{dP}\frac{d\lambda_r}{dn_{eff}}\frac{dT}{d\lambda_r}$$

T:**transmission through the bus waveguide** P: **ultrasoniic pressure**

λ_r: **resonance wavelength** n_{eff}: **effective refractive index**

$$m\lambda_r = 2\pi R n_{eff}, \quad \frac{d\lambda_r}{dn_{eff}} = \frac{2\pi R}{m} = \frac{\lambda_r}{n_{eff}}$$

$$S = A\lambda_r Q$$

A: design-specific parameter

Q: Q-factor

Setup

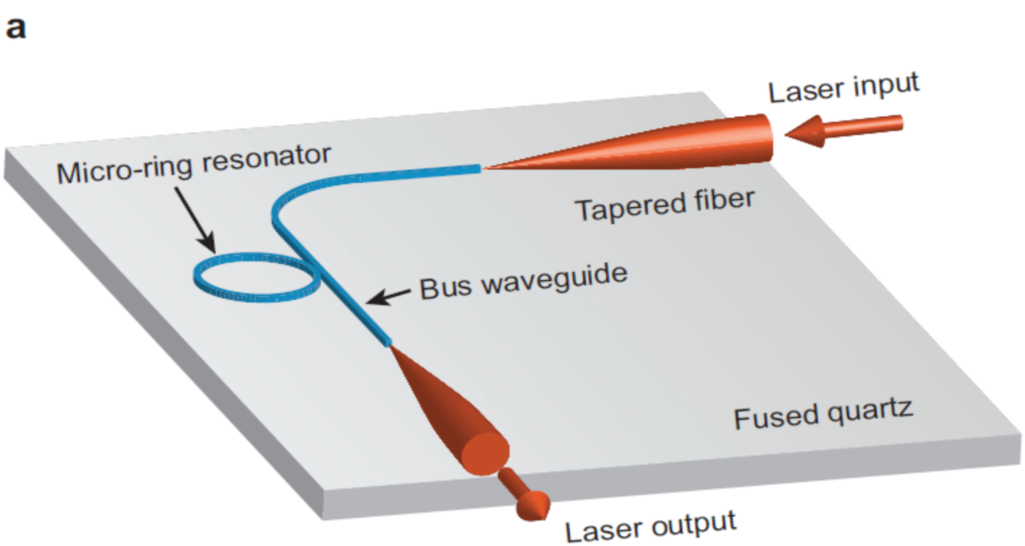

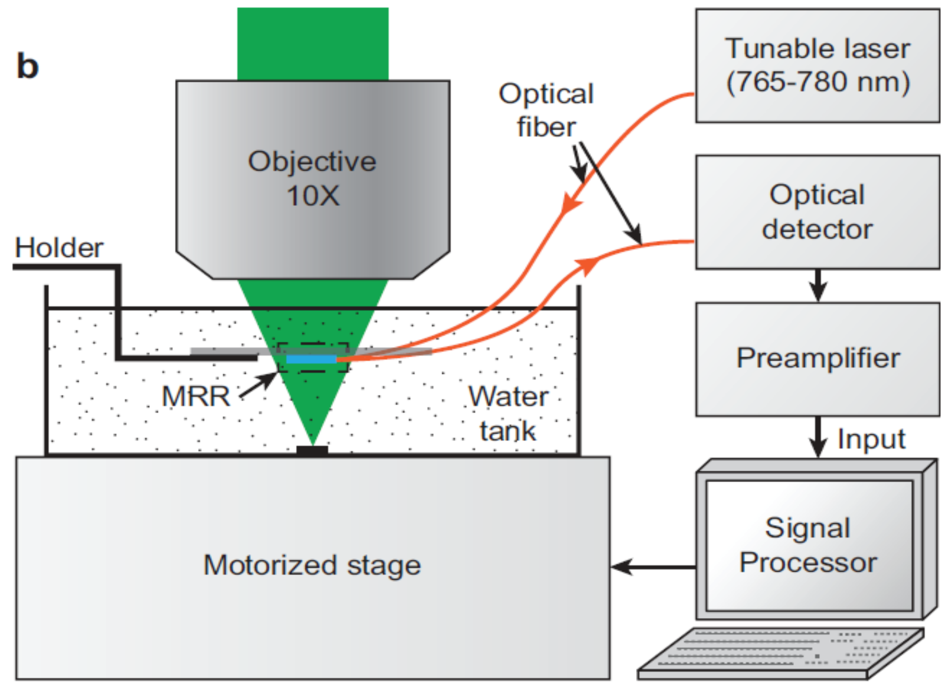

They characterized the frequency-dependent sensitivity of the MRR ultrasound detector using a PA point source

PA point source:1.5μm thick carbon black thin film

Impulse responsee of the MRR based PAM system

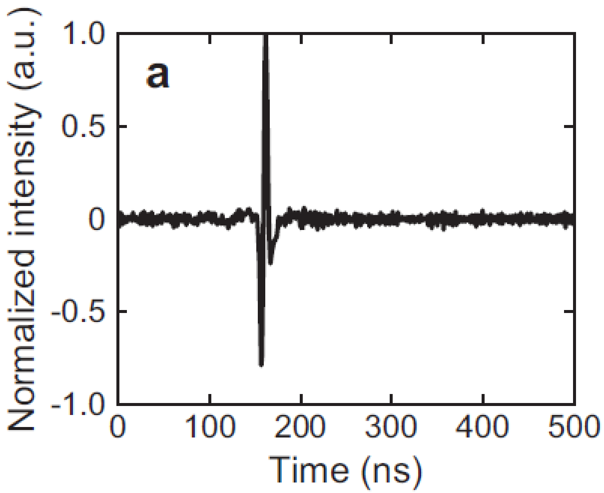

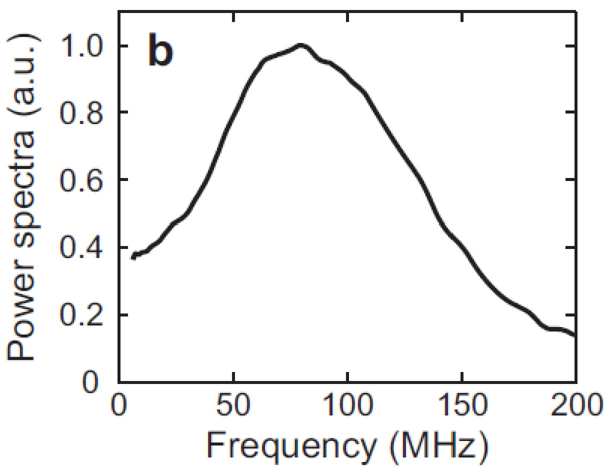

Noise level 0.32mV

Noise equivalent pressure 6.8Pa

The NEP obtained from this study is several orders of magnitude better than conventional piezoelectric transducers with comparable size

3dB bandwidth of 140MHz

Comparison of PA saturation limits

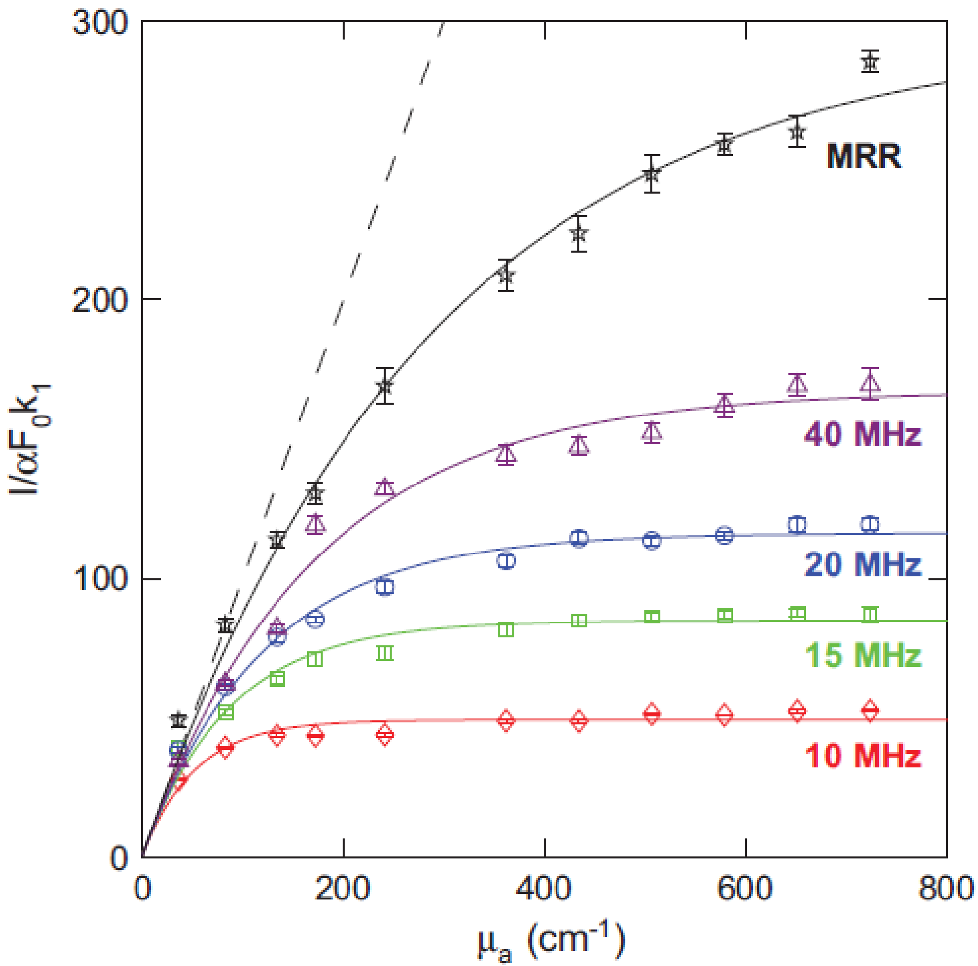

Angular dependence of the frequency response of the MRR ultrasonic detector

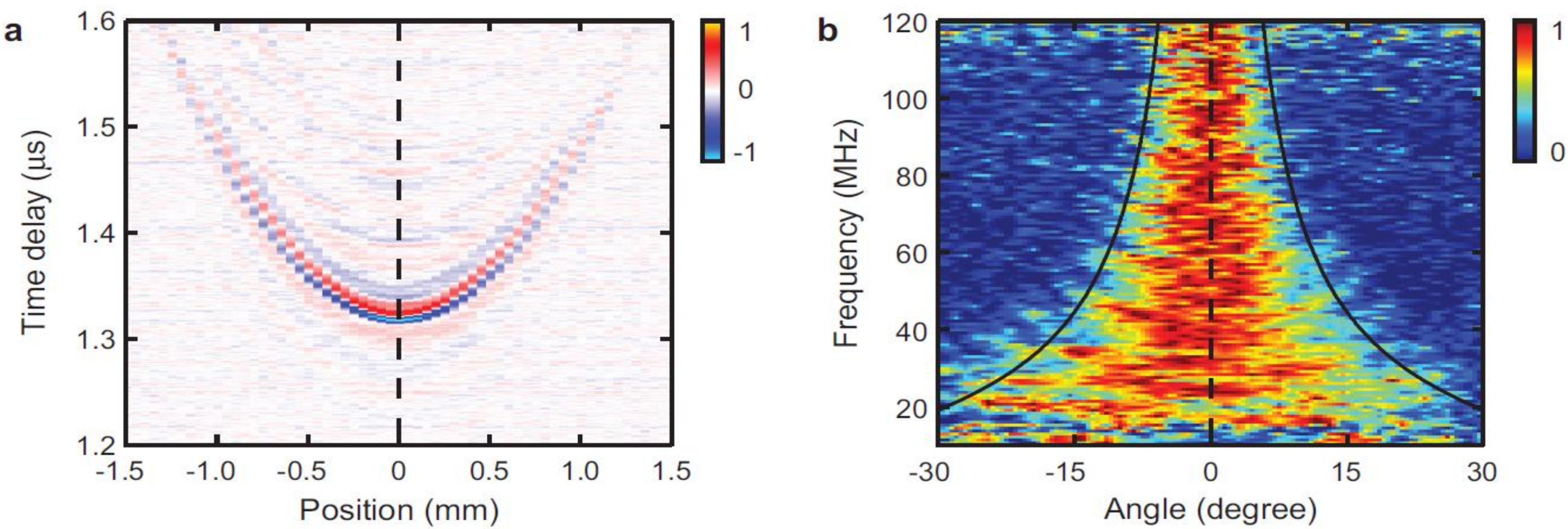

The lateral and axial resolutions

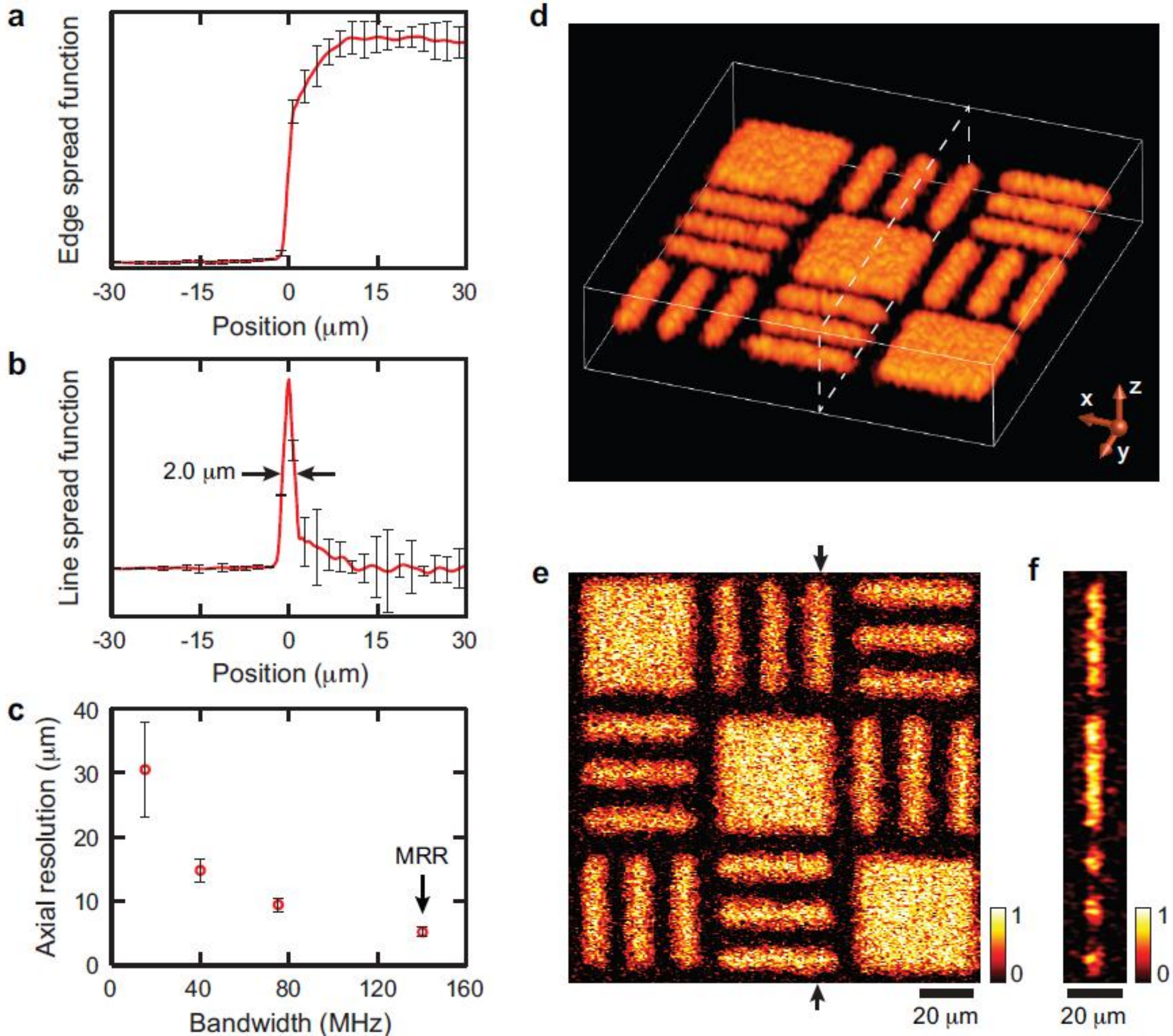

Summary

1) the MRR ultrasonic detector is fully compatible with microscopic imaging systems and can be used with **high-NA objective lenses**

2) an **axial resolution of 5.3 mm** has been obtained experimentally as a result of the MRR's ultra-wide frequency response

3) there can be **a nearly two-fold improvement in the PA saturation limit** compared with piezoelectric detectors

光音響法

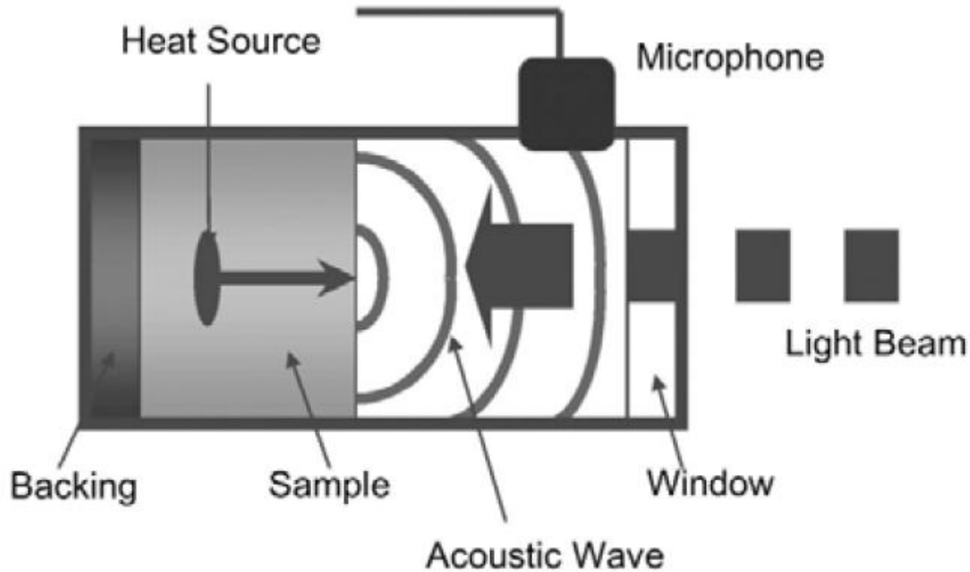

図１．光音響シグナル発生のメカニズム

Single-shot acoustic waveform measured by the resonator

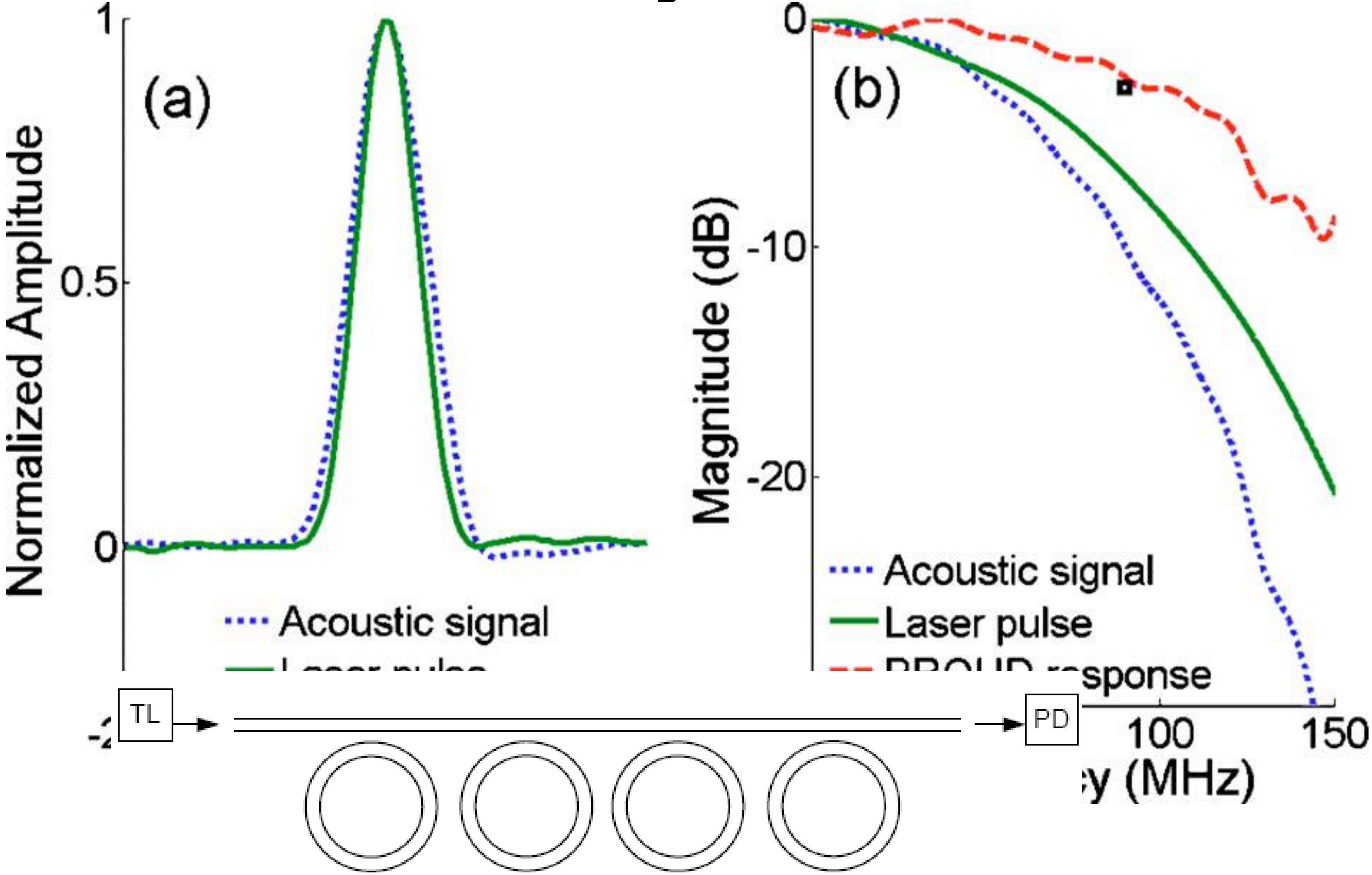

(a)

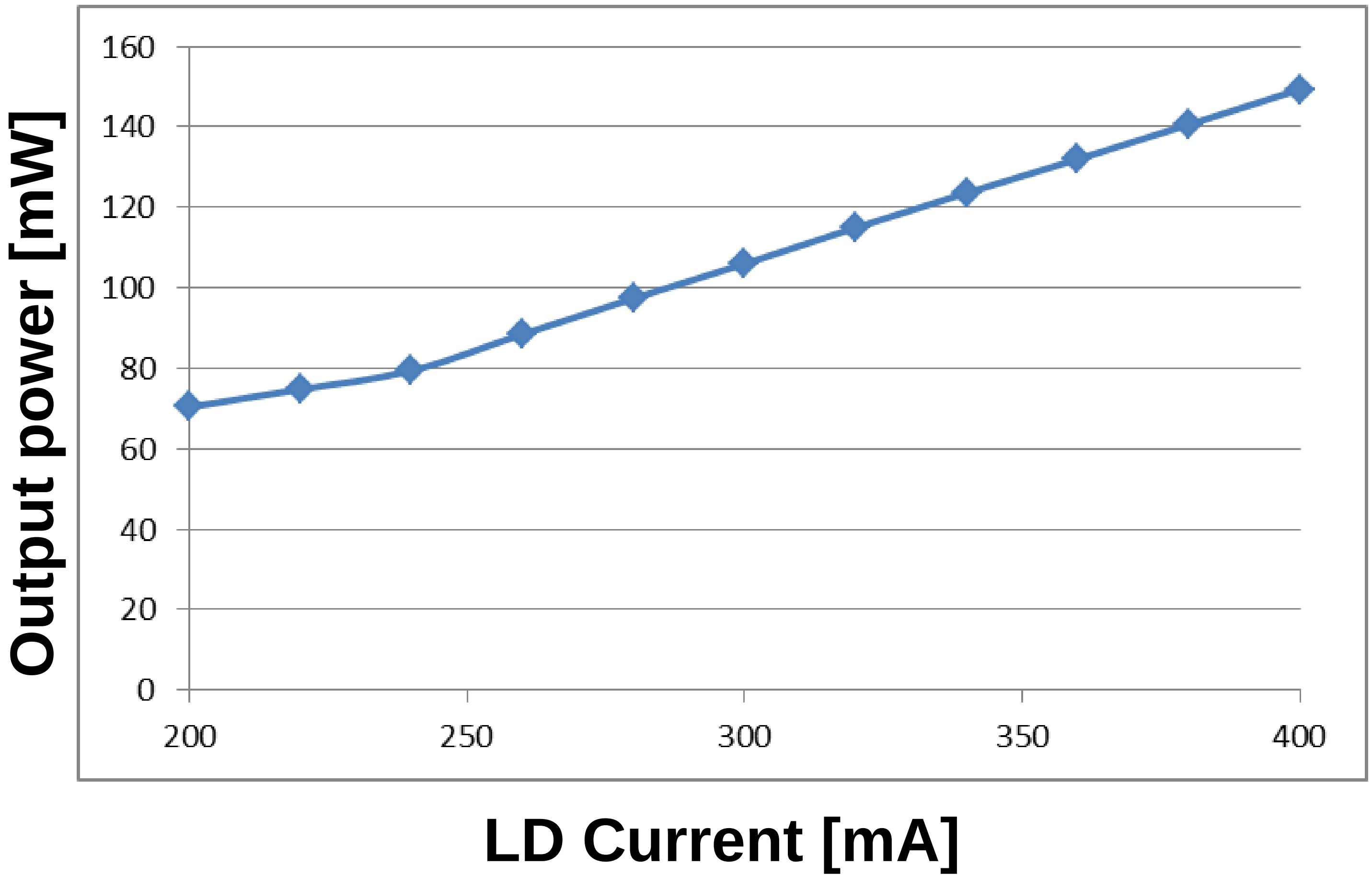
Output power [mW]
160
140
120
100
80
60
40
20
0
200
250
300
350
400
LD Current [mA]